

Explainable deep learning improves human mental models of self-driving cars

Eoin M. Kenny^{1*}, Akshay Dharmavaram², Sang Uk Lee²,
Tung Phan-Minh², Shreyas Rajesh², Yunqing Hu², Laura Major²,
Momchil S. Tomov^{2,3†}, Julie A. Shah^{1,4†}

¹Computer Science & Artificial Intelligence Laboratory (CSAIL),
Massachusetts Institute of Technology, Cambridge, MA, USA.

² Motional AD Inc., Boston, MA, USA.

³Department of Psychology and Center for Brain Science, Harvard
University, Cambridge, MA, USA.

⁴Department of Aeronautics and Astronautics, Massachusetts Institute
of Technology, Cambridge, MA, USA.

*Corresponding author(s). E-mail(s): ekenny@mit.edu;

Contributing authors: momchil.tomov@motional.com;

julie.a.shah@csail.mit.edu;

†These authors contributed equally to this work.

Summary

Self-driving cars increasingly rely on deep neural networks to achieve human-like driving [1–3]. The opacity of such black-box planners makes it challenging for the human behind the wheel to accurately anticipate when they will fail [4–6], with potentially catastrophic consequences [7–9]. While research into interpreting these systems has surged, most of it is confined to simulations or toy setups due to the difficulty of real-world deployment [10, 11], leaving the practical utility of such techniques unknown. Here, we introduce the Concept-Wrapper Network (CW-Net), a method for explaining the behavior of machine-learning-based planners by grounding their reasoning in human-interpretable concepts. We deploy CW-Net on a real self-driving car and show that the resulting explanations improve the human driver’s mental model of the car, allowing them to better predict its behavior. To our knowledge, this is the first demonstration that explainable deep learning integrated into self-driving cars can be both understandable and useful in a realistic deployment setting. CW-Net accomplishes this level of intelligibility while providing explanations which are causally faithful and do not sacrifice

driving performance. Overall, our study establishes a general pathway to interpretability for autonomous agents by way of concept-based explanations, which could help make them more transparent and safe.

Keywords: Self-driving cars, Mental models, Situational awareness, Interpretable ML

1 Introduction

There are hundreds of companies developing autonomous vehicle (AV) technology globally [12], promising to revolutionize transportation for everyone. The industry currently spans two segments: driverless ride-hail systems and consumer vehicles [13]. In consumer vehicles, machine learning (ML) solutions have markedly improved advanced driver-assistance systems, yet they still require human intervention in unusual or challenging situations where learned planners may not determine the correct action [14]. As driving is safety-critical, such infrequent failures matter, making it essential that the human driver is able to anticipate and be prepared for such situations [15]. However, the opaque nature of ML planners makes it challenging to interpret and communicate the causes of their decisions, hampering the ability of human drivers to understand and predict AV behavior while achieving real-time situational awareness [16–18].

Lack of effective communication between the AV and the human driver has contributed to multiple high-profile incidents, some resulting in fatalities [7–9], highlighting the urgent need to make ML planners interpretable [11]. Previous studies have sought to address this using surveys and simulated scenarios [19–26], a human driver emulating the AV [27, 28], or large language models providing post-hoc explanations [3]. However, these studies were theoretical, did not provide causally faithful explanations, were only evaluated in simulation, or did not convincingly show the practical utility of the explanations. This leaves open the question of how to provide explanations that are understandable, useful, and faithful to the decision-making process of the AV in a realistic setting.

To answer this question, we scale up our recent work on interpretable-by-design deep reinforcement learning [10] using motifs from the literature on concept-bottleneck models [29] to propose the Concept-Wrapper Network (CW-Net). CW-Net grounds the reasoning of a black-box ML planner in human-interpretable concepts, such as “Approaching stopped vehicle” or “Close to cyclist”. This method is rooted in case-based reasoning, a classical artificial intelligence (AI) approach [30–32] inspired by cognitive models of human reasoning and memory [33]. CW-Net can be applied to arbitrary pretrained deep neural networks, does not require retraining from scratch, and does not degrade the performance of the original black-box ML planner. Since the inferred concepts are the sole input to the final decision-making module of CW-Net that directly dictates AV behavior, we refer to them as *causally faithful explanations*.

We apply CW-Net to a ML planner trained to imitate human driving behavior using inverse reinforcement learning [1, 2]. We replace the final (reward) layer of the pretrained deep neural network with a concept classifier, followed by a new reward layer. We then jointly train the classifier and the new reward layer to predict

scenario types and driving decisions, respectively, without modifying the rest of the network. Evaluation on a large-scale benchmark [10] confirms that CW-Net is able to classify concepts without compromising driving behavior. To study the utility of the explanations, we deploy CW-Net on a real self-driving car with a safety driver in a semi-naturalistic study [35]. We demonstrate three situations in which the driver’s initially inaccurate mental model is subsequently improved by the CW-Net explanations, which in turn allows the driver to more accurately predict AV behavior. We then observe similar mental model improvement in a larger online study simulating these scenarios. Lastly, we link these results to more complex real-world scenarios by deploying CW-Net on public roads in Las Vegas. We use these new data in a large online study ($N = 100$) to demonstrate that improvements in mental model goodness lead to improved predictive ability and situational awareness. Overall, our work demonstrates how explainable AI can help users of an advanced autonomous system improve their mental model of the system and better anticipate its future behavior.

2 Black-box planner

We focus on the planning module of the AV stack (Figure 1a), which takes as input a scene context s and outputs a trajectory $\hat{\tau}$. Here, s is a symbolic object-oriented representation of the scene, computed by the perception module, while $\hat{\tau}$ is the trajectory that the subsequent controller module should follow. We use a deep neural network architecture [1, 2] consisting of a scene encoder $H(s) \rightarrow \mathbf{h}$ and a trajectory generator $G(s) \rightarrow \{\tau_1 \dots \tau_k\}$, followed by a scene-trajectory encoder $E(\mathbf{h}, \tau_i) \rightarrow \mathbf{z}_i$ and a final reward layer $R(\mathbf{z}_i) \rightarrow r_i$ (Figure 1b). H computes a scene embedding \mathbf{h} and G computes a set of k candidate trajectories $\{\tau_1 \dots \tau_k\}$. Those are combined in E to compute an embedding \mathbf{z}_i for each trajectory τ_i . Finally, R computes an estimated reward r_i for each trajectory τ_i , quantifying how human-like it is. In other words, r_i is higher when τ_i is more similar to how a human would drive in this situation.

During inference, the trajectory with highest reward is selected on each iteration:

$$\hat{\tau} = \arg \max_{\tau \in \{\tau_1 \dots \tau_k\}} R(E(\mathbf{h}, \tau))$$

We use inverse reinforcement learning to train the planner on 80 hours of human expert driving [1, 2].

3 Planning over human-friendly concepts

To make the ML planner interpretable, we modify the planner architecture to additionally provide explanations for its behavior [10]. Our working definition of explainable AI follows Gunning & Aha [36], who define it as ‘*AI systems that can explain their rationale to a human user, characterize their strengths and weaknesses, and convey an understanding of how they will behave in the future.*’

Specifically, we replace R with a concept classifier $C(\mathbf{z}_i) \rightarrow \mathbf{c}_i$, followed by a new reward layer $R'(\mathbf{c}_i) \rightarrow r'_i$ (Figure 1c). The concept classifier C computes a logit vector \mathbf{c}_i that is passed through a softmax and/or sigmoid layer that, in turn, assigns probabilities to different human-interpretable concepts. Since R' computes trajectory

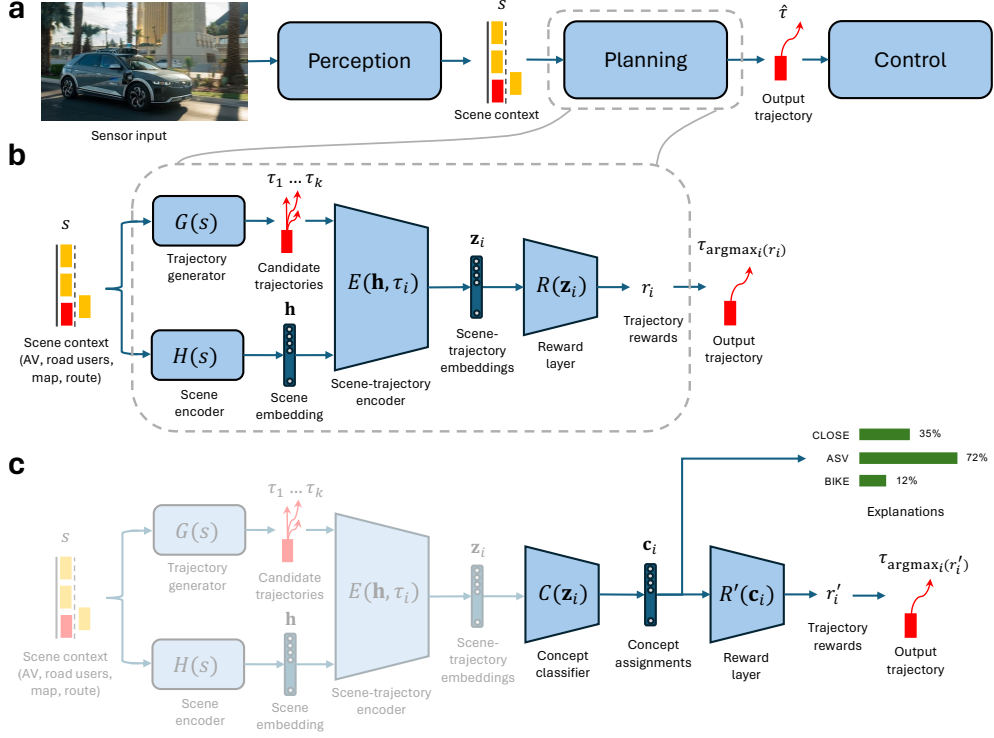


Fig. 1 Planner architecture, adapted with permission from Tomov et al. (2025) [1]. **a.** Autonomous vehicle stack. Sensory input is processed by the perception module to generate scene context s . The planning module processes s to compute trajectory $\hat{\tau}$, which is followed by the control module. **b.** Black-box ML planner. Here, s is fed to trajectory generator G , which produces candidate trajectories $\{\tau_1 \dots \tau_k\}$, and scene encoder H , which produces a scene embedding h . These are fed into encoder E , which produces scene-trajectory embeddings z_i for each τ_i , which are in turn fed into the reward layer R . R computes a reward r_i for each trajectory. The model is trained to output higher rewards for trajectories closer to the the ground-truth human trajectories. **c.** CW-Net. Identical to **b.**, except z_i is fed to a concept classifier C , which produces concept assignments c_i . These are fed to a new reward layer R' to produce rewards r'_i . In parallel, c_i is processed to generate the explanations. The reward layer is trained to prefer the same trajectories as the black-box ML planner, while the concept layer is supervised with ground-truth scenario labels. The weights of the faded components are frozen during training. CLOSE, “Close to another vehicle”. ASV, “Approaching stopped vehicle”. BIKE, “Close to cyclist”.

rewards from c_i , the final decisions are based solely on these concept assignments and hence they constitute a causally faithful explanation. The rest of the network remains the same.

Similarly to the black-box planner, trajectories are selected according to:

$$\hat{\tau} = \arg \max_{\tau \in \{\tau_1 \dots \tau_k\}} R'(C(E(h, \tau)))$$

We train CW-Net to jointly predict concept labels and mimic the driving decisions of the black-box planner. Specifically, c_i is supervised with labels corresponding

to types of scenarios, such as “Approaching stopped vehicle” or “Close to cyclist” (see Section 8.5 for a full list of concepts). This ensures that CW-Net assigns a unique interpretable concept to each unit in \mathbf{c}_i . At the same time, r'_i is supervised with trajectories selected by the black-box planner using a cross-entropy loss. During training, the rest of the deep neural network (H , G , and E) is kept frozen (see Section 8.2 for more details). We focus our study on this particular ML planner architecture, noting that prior work indicates CW-Net would generalize effectively to other architectures [10].

4 Classifying concepts while preserving planner performance

As a baseline, we first evaluated the black-box planner (without CW-Net) using closed-loop simulations with the nuPlan simulator on the nuPlan dataset [10] (Table S1). Overall, the results were competitive with the top submissions to the nuPlan challenge, although performance was slightly lacking when starting from a stop (see Section 8.5). This suggests that there is room for improvement and, importantly, opportunities to study explanations of undesirable behavior.

We then evaluated the driving performance of CW-Net wrapped around the black-box planner (Table S1). The results were equivalent, with less than 1% difference across all metrics, confirming that our method did not degrade driving performance. We also evaluated concept classification on held-out datasets (Tables S2, S3). Mean accuracy was 54%, with 23% precision, 77% recall, and an F1 score of 0.31 (see Section 8.3). Overall, these results indicate that CW-Net can be used to ground the decision making of high-performance ML planners in human-interpretable concepts, without sacrificing driving performance.

5 Mental model improvement in surprising real-world situations

Our central hypothesis is that the explanations from CW-Net would improve the human driver’s mental model of the AV and, by extension, their situational awareness. This would be particularly salient in surprising situations, which is when explanations are most useful [37]. Specifically, the explanations should improve the driver’s ability to understand and address the reasons for AV failures, and also to predict its future behavior.

To test this hypothesis, we deploy CW-Net on a real AV on a private track using the Lab2Car wrapper [35] and observe how safety drivers react to surprising events and the corresponding CW-Net explanations (Figure 2). These situations were not planned, but instead occurred naturally, with minimal intervention from the researchers, who only dictated high-level plans for each day. This semi-naturalistic study allowed us to assess the utility of the explanations in naturally occurring surprising situations. To measure AV predictability, we record the drivers’ ability to make counterfactual predictions about AV behavior in these situations. To note the drivers’ mental models, together with their predictive ability, we additionally record their think-aloud thoughts



Fig. 2 Deployment setup. A safety driver, a support engineer, and a researcher were present. The safety driver drove the AV manually between road tests, engaged self-driving mode at the start of each test, monitored AV performance during the test, and took over in case of unsafe driving. The support engineer deployed CW-Net and set scenario destinations. The researcher directed testing. The dashboard included a map with overlaid object detections (s) from the perception module and the output trajectory ($\hat{\tau}$). Explanations c_i from CW-Net were shown as percentages for easier interpretation [39].

before and after considering CW-Net explanations [11]. We focus on concepts that relate to other road users and can be easily tested counterfactually (see Section 8.5).

5.1 Unexpected stopping for nearby vehicles

We observed that the AV repeatedly came to a stop shortly before a pedestrian pickup/drop-off zone (Figure 3a). The driver’s intuition was that the car stopped because of the pickup/drop-off zone, but the explanations indicated that the planner stopped because it detected that it was “*Close to another vehicle*” (the CLOSE concept). To test this hypothesis, the driver manually moved the car farther from the parked cars. At this point, the probability of CLOSE decreased and the AV began moving again, thus supporting the alternative hypothesis. A full timeline of events is detailed in Figure 3a. We fitted the intercept of the CLOSE probability against the speed of the AV globally and found it accurately predicts stopping and starting for this event.

5.2 Hallucinating a stopped vehicle ahead

At another location, the AV would reliably come to a stop next to a traffic cone (Figure 3b). The driver’s initial mental model was that the cone was responsible for the phantom brake. However, the “*Approaching stopped vehicle*” (ASV) concept peaked shortly before the car stopped. This suggested an alternative hypothesis, that the planner matched the current situation with training scenarios labeled ASV, which in turn promotes stopping behavior associated with such scenarios. As a counterfactual test, the cone was removed. The AV exhibited the same stopping behavior at the same location, along with similar ASV probability and speed profiles (L_2 similarities of 1.12 and 1.6 between the respective time-warped profiles, compared to an average $L_2 > 200$ for random events), thus supporting the alternative hypothesis. Note that although there was no vehicle in front of the AV, the explanation is causally faithful to the underlying planner and explains why it stopped (namely, because it incorrectly

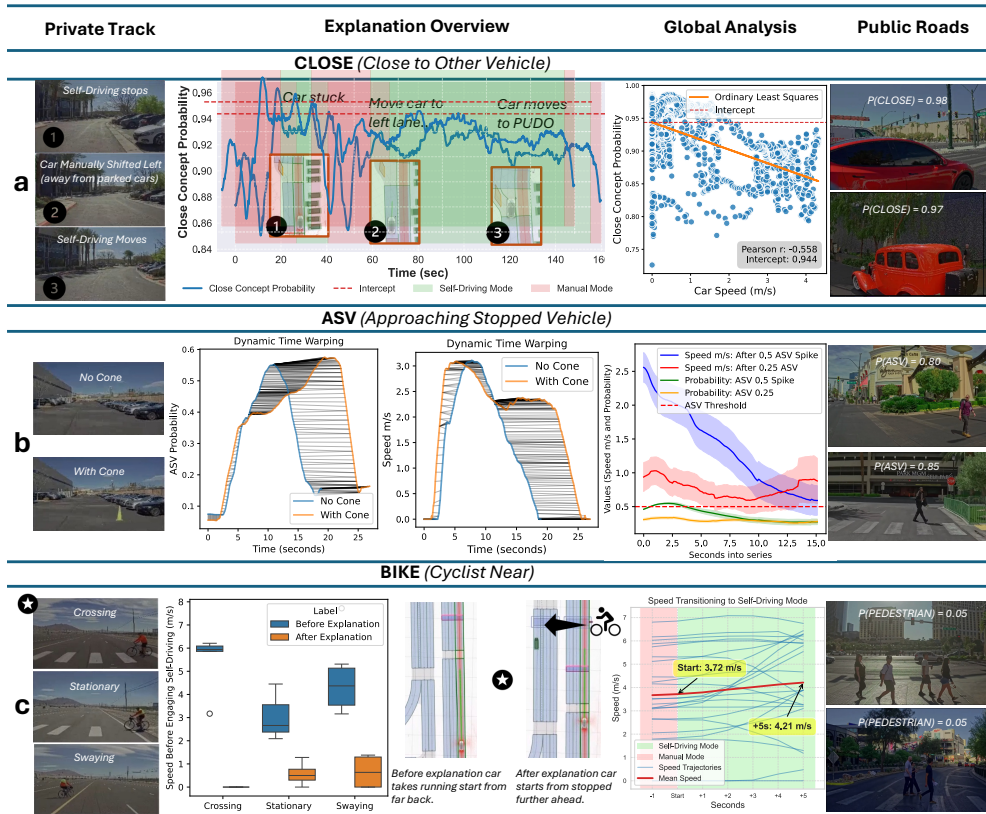


Fig. 3 Results: **a.** The CLOSE concept activated when the car got stuck next to parked vehicles. The driver initially thought the pickup/drop-off area was the cause, but the explanation suggested that it was the nearby vehicles. When the driver engaged self-driving away from the park vehicles, activation of the CLOSE concept decreased and the AV started moving again, counter to driver’s initial mental model and consistent with the explanations. Across tests, CLOSE correlated with speed and the intercept accurately predicted this event. **b.** The ASV concept activated when the car stopped next to a traffic cone. The driver initially thought the cone was the cause, but the explanation suggested that the AV was hallucinating a stopped vehicle. When we removed the cone in a counterfactual test, the same phantom braking and concept activation occurred. Across tests, ASV correlated with reductions in speed when spiking above 0.5 probability. **c.** The BIKE concept failed to activate in our first round of tests with a cyclist, but the car always stopped safely for the cyclist. After observing the explanation, the driver engaged self-driving from slower speeds in a second round of tests. Follow-up analyses revealed that the AV stopped for the cyclist due to backup safety mechanisms unrelated to CW-Net, which indicates that the driver’s increased level of caution was appropriate. **a-c.** (Right column) Naturalistic scenarios from public-road deployment, analogous to the scenarios observed on the private track. We used the PEDESTRIAN concept instead of the BIKE concept as it behaved similarly and pedestrians were more frequently encountered on public roads. Likewise, we used pedestrians in place of the traffic cone in our ASV tests as there were no cones encountered on the public roads. Standard error of the mean and 3-second rolling averages are shown in relevant plots.

detected a stopped vehicle). Figure 3b illustrates a global analysis of ASV, showing it to be a powerful predictor of braking.

5.3 Reacting safely to cyclist

Finally, we tested the ability of the AV to stop safely for cyclists (Figure 3c). For each test, the driver engaged self-driving mode while approaching a cyclist. The driver was instructed to engage self-driving from a speed at which they felt safe, since this determines the subsequent speed of the AV. During the initial tests, the AV reliably stopped for the cyclist. However, the BIKE concept maintained a low probability throughout each test ($< 1\%$), indicating that CW-Net was failing to detect the cyclist. Over time, the driver became aware of the concept reading and gradually increased their caution by initiating self-driving from slower speeds. A post-hoc analysis revealed that, although the perception system detected the cyclist, the ML planner was not configured to consume inputs for cyclists. As a result, it chose unsafe trajectories which would have collided with the cyclist. In reality, the AV stopped due to a built-in safety backup system, which commands a brake if collision is imminent. This indicates that the increased caution dictated by the driver’s updated mental model was warranted.

6 Mental model improvement in simulation studies

The semi-naturalistic study above illustrates how CW-Net explanations can improve the human driver’s mental model of the AV in surprising real-world situations, leading to better understanding and predictability of AV behavior. To validate that these results replicate in larger populations and generalize to naturalistic scenarios, we conduct several larger follow-up studies (Figures S2, S3). First, we show that in simulations of the real-world scenarios in Section 5, CW-Net explanations consistently improve mental models and predictions for both experts and non-experts alike. Second, we collect data from CW-Net in naturalistic real-world scenarios on public roads and show that the explanations improve situational awareness – an indirect measure of mental model goodness [12] – in surprising situations, without degrading it in unsurprising situations.

6.1 Explanations improve mental models and predictability

The purpose of the first study is to (1) demonstrate that the effects observed on the road reproduce in larger populations, and (2) establish a link between direct measures of mental model goodness and performance on downstream tasks, such as predicting AV behavior. We conducted an online survey in which we showed participants replays of the scenarios from the private track (front camera recordings with overlaid CW-Net explanations; Figure S11).

For each scenario, we asked participants to choose the reason for AV behavior that best aligns with their current beliefs (i.e., “*Why did the AV do that?*”) and to make counterfactual predictions (i.e., “*What would the AV do if ...?*”). Following Hoffman et al. [11], we refer to the former as the *nearest-neighbor task* – since it forces participants to pick the nearest explanation to their beliefs – and the latter as the *prediction task*. Both tasks consist of a multiple-choice question followed by a confidence score. The prediction task additionally includes a free-form text response where participants can describe the reasons for their prediction. The nearest-neighbor

task and the free-form text response directly probe the participants’ mental models, while the multiple-choice prediction question serves as a proxy performance metric for mental model goodness. Critically, we collected responses before and after observing the explanations. This within-subject design mirrors the experience of drivers during the real-world tests (Figures S2, S3). The study was conducted with experts ($N = 9$ Motional drivers/engineers) and non-experts ($N = 30$ pseudo-random participants from Prolific.com).

On the nearest-neighbor task, CW-Net explanations improved mental models for almost all participants (8/9 experts and 27/30 non-experts; Figure S4). Free-form text responses were initially similar to the initial beliefs of the safety drivers during the on-road tests ($p < 10^{-9}$) and then shifted towards their final beliefs ($p < 0.0002$) and the ground-truth reasons for AV behavior ($p < 10^{-5}$; exact binomial tests for non-experts; Figures S6, S7). The distribution of mental model updates on both tasks was similar across both groups ($\beta = 0.04, p = 0.8$, ordinary least-squares regression; Figure S8). Importantly, mental model improvement on the nearest-neighbor task correlated with improvements in prediction accuracy ($\beta = 2.02 \pm 0.87, p = 0.02$ for experts, $\beta = 9.86 \pm 2.07, p < 0.001$ for non-experts; linear mixed-effects models [LMEs]; Figure S9, left). A similar effect was observed for the free-form text responses ($\beta = 1.70 \pm 0.91, p = 0.06$ for experts, $\beta = 5.03 \pm 1.23, p < 0.001$ for non-experts; LMEs; Figure S9, right). Together, these results support the conclusion that CW-Net explanations can reliably improve mental models of the AV and that prediction performance can serve as a reliable proxy for mental model goodness.

6.2 Explanations improve situational awareness in naturalistic scenarios

To verify that the effects observed on the private track generalize to more complex, naturalistic scenarios, we deployed CW-Net on public roads in Las Vegas (Figures S3; Figure 3, right). Due to safety reasons and the experimental nature of the ML planner, the safety driver operated the AV in ‘manual’ mode for several hours, with CW-Net running in the background. This allowed us to collect naturalistic scenarios analogous to those encountered on the private track [28, 41] (Figure S10). We use replays of those scenarios to conduct a large-scale online study ($N = 100$) within the Situation Awareness Global Assessment Technique (SAGAT) framework tailored for explainable AI [12, 42].

The SAGAT framework is the gold standard for evaluating situational awareness in complex, dynamic tasks [12, 42]. It measures the situational awareness of a human operator by freezing a scenario, querying the operator about their *perception* (i.e., “What are the inputs to the AV?”), *comprehension* (i.e., “Why is the AV doing that?”), and *projection* (i.e., “What would the AV do if ...?”) of the situation (Figure S11) and comparing their responses with the ground truth. As counterfactual predictive performance in Section 6.1 aligns with mental model goodness, we use projection in SAGAT as a proxy for mental model elicitation and quality [11]. For each type of scenario and corresponding concept, we sample two instances in which AV behavior was surprising (e.g., stopping unnecessarily) and two corresponding instances in which it was unsurprising (Table S6). We use a between-subject design in which the experimental group

received explanations from CW-Net, while the control group received placeholder explanations of AV kinematics to balance cognitive load [14] (Figures S12-S14).

We found that the CW-Net explanations significantly improved measures of situational awareness for surprising events (Figure S15, left; Table S7, top), with large effect sizes for perception (Cohen’s $d = 1.290$), comprehension (Cohen’s $d = 0.996$), and a medium effect size for projection (Cohen’s $d = 0.606$). Conversely, explanations did not impact situational awareness for unsurprising events (Figure S15, right; Table S7, bottom). Together, these results show that the explanations from CW-Net are robust across various conditions and can reliably improve mental models in surprising situations, without significant negative effects in unsurprising situations. Moreover, they demonstrate pragmatic usage of the improved mental models.

7 Conclusion

Our work shows, for the first time, how explainable deep learning can provide useful explanations for AVs in a real-world setting. CW-Net achieves this by grounding the reasoning of a pretrained black-box ML planner in human-interpretable concepts that are directly used to make driving decisions. By revealing otherwise inaccessible information about the decision-making process of the AV in real time, CW-Net helps improve the human driver’s mental model of the AV. This, in turn, improves the driver’s situational awareness and reveals limitations of the robotic system, helping the driver better anticipate its mistakes.

Many systems involving human-robot interaction require real-time explanations, and many of these applications increasingly rely on deep learning, with a long tail of potentially catastrophic failure cases. Indeed, many regulatory bodies have already made explainable AI a core component of their legislation, with AVs likely to follow suit as they are widely deployed with various users [11]. As such, the success of CW-Net suggests that similar algorithms may prove essential for meeting the regulatory standards for deploying AVs, while building appropriate trust in the technology. In future work, it would be prudent to extend CW-Net to cover a larger set of concepts – perhaps in an unsupervised manner to overcome the challenges of labeling – to better cover the vast array of concepts relevant to AV settings.

References

- [1] Momchil S. Tomov, Sang Uk Lee, Hansford Hendrigo, Jinwook Huh, Teawon Han, Forbes Howington, Rafael da Silva, Gianmarco Bernasconi, Marc Heim, Samuel Findler, Xiaonan Ji, Alexander Boule, Michael Napoli, Kuo Chen, Jesse Miller, Boaz Floor, and Yunqing Hu. Treeirl: Safe urban driving with tree search and inverse reinforcement learning. 2025.
- [2] Tung Phan-Minh, Forbes Howington, Ting-Sheng Chu, Momchil S Tomov, Robert E Beaudoin, Sang Uk Lee, Nanxiang Li, Caglayan Dicle, Samuel Findler, Francisco Suarez-Ruiz, et al. Driveirl: Drive in real life with inverse reinforcement learning. In *2023 IEEE International Conference on Robotics and Automation (ICRA)*, pages 1544–1550. IEEE, 2023.

- [3] Ana-Maria Marcu, Long Chen, Jan Hünermann, Alice Karnsund, Benoit Hanotte, Prajwal Chidananda, Saurabh Nair, Vijay Badrinarayanan, Alex Kendall, Jamie Shotton, et al. Lingoqa: Video question answering for autonomous driving. *arXiv preprint arXiv:2312.14115*, 2023.
- [4] Stefanos Nikolaidis and Julie Shah. Human-robot teaming using shared mental models. *ACM/IEEE HRI*, 2012.
- [5] Laura Major and Julie Shah. *What to expect when you're expecting robots: the future of human-robot collaboration*. Hachette UK, 2020.
- [6] Rohan Paleja, Muyleng Ghuy, Nadun Ranawaka Arachchige, Reed Jensen, and Matthew Gombolay. The utility of explainable ai in ad hoc human-machine teaming. *Advances in neural information processing systems*, 34:610–623, 2021.
- [7] James Titcomb. Uber’s safety policies under fire as us watchdog investigates self-driving car death, 11 2019.
- [8] Lee Fang. Tesla crash footage shows driver with hands off wheel, raising fresh questions about autopilot safety, 1 2023.
- [9] Brad Templeton. Waymo’s double crash with pickup trucks and more examined. *Forbes*, 2024. Accessed: 2024-09-22.
- [10] Eoin M Kenny, Mycal Tucker, and Julie Shah. Towards interpretable deep reinforcement learning with human-friendly prototypes. In *The Eleventh International Conference on Learning Representations*, 2023.
- [11] Shahin Atakishiyev, Mohammad Salameh, Hengshuai Yao, and Randy Goebel. Explainable artificial intelligence for autonomous driving: A comprehensive overview and field guide for future research directions. *IEEE Access*, 2024.
- [12] Claudine Badue, Rânik Guidolini, Raphael Vivacqua Carneiro, Pedro Azevedo, Vinicius B Cardoso, Avelino Forechi, Luan Jesus, Rodrigo Berriel, Thiago M Paixao, Filipe Mutz, et al. Self-driving cars: A survey. *Expert systems with applications*, 165:113816, 2021.
- [13] Taxonomy and definitions for terms related to driving automation systems for on-road motor vehicles. Technical Report SAE J3016, SAE International, Warrendale, PA, 2021. Revised June 2021.
- [14] Yang Xing, Chen Lv, Dongpu Cao, and Peng Hang. Toward human-vehicle collaboration: Review and perspectives on human-centered collaborative automated driving. *Transportation research part C: emerging technologies*, 128:103199, 2021.
- [15] Ana Pereira and Carsten Thomas. Challenges of machine learning applied to safety-critical cyber-physical systems. *Machine Learning and Knowledge*

Extraction, 2(4):579–602, 2020.

- [16] Anton Kuznietsov, Balint Gyevnar, Cheng Wang, Steven Peters, and Stefano V Albrecht. Explainable ai for safe and trustworthy autonomous driving: A systematic review. *IEEE Transactions on Intelligent Transportation Systems*, 2024.
- [17] Selene Arfini, Pierstefano Bellani, Andrea Picardi, Ming Yan, Fabio Fossa, and Giandomenico Caruso. Design for inclusivity in driving automation: theoretical and practical challenges to human-machine interactions and interface design. In *Connected and Automated vehicles: integrating engineering and ethics*, pages 63–85. Springer, 2023.
- [18] Shahin Atakishiyev, Mohammad Salameh, and Randy Goebel. Incorporating explanations into human-machine interfaces for trust and situation awareness in autonomous vehicles. In *2024 IEEE Intelligent Vehicles Symposium (IV)*, pages 2948–2955. IEEE, 2024.
- [19] Jeamin Koo, Jungsuk Kwac, Wendy Ju, Martin Steinert, Larry Leifer, and Clifford Nass. Why did my car just do that? explaining semi-autonomous driving actions to improve driver understanding, trust, and performance. *International Journal on Interactive Design and Manufacturing (IJIDeM)*, 9:269–275, 2015.
- [20] Jeamin Koo, Dongjun Shin, Martin Steinert, and Larry Leifer. Understanding driver responses to voice alerts of autonomous car operations. *International journal of vehicle design*, 70(4):377–392, 2016.
- [21] Gesa Wiegand, Malin Eiband, Maximilian Haubelt, and Heinrich Hussmann. “i’d like an explanation for that!” exploring reactions to unexpected autonomous driving. In *22nd International Conference on Human-Computer Interaction with Mobile Devices and Services*, pages 1–11, 2020.
- [22] Chao Wang, Thomas H Weisswange, Matti Krueger, and Christiane B Wiebel-Herboth. Human-vehicle cooperation on prediction-level: Enhancing automated driving with human foresight. In *2021 IEEE Intelligent Vehicles Symposium Workshops (IV Workshops)*, pages 25–30. IEEE, 2021.
- [23] Tobias Schneider, Sabiha Ghellal, Steve Love, and Ansgar RS Gerlicher. Increasing the user experience in autonomous driving through different feedback modalities. In *26th International Conference on Intelligent User Interfaces*, pages 7–10, 2021.
- [24] Tobias Schneider, Joana Hois, Alischa Rosenstein, Sabiha Ghellal, Dimitra Theofanou-Fülbiér, and Ansgar RS Gerlicher. Explain yourself! transparency for positive ux in autonomous driving. In *Proceedings of the 2021 CHI Conference on Human Factors in Computing Systems*, pages 1–12, 2021.

- [25] Daniel Omeiza, Helena Web, Marina Jirotko, and Lars Kunze. Towards accountability: providing intelligible explanations in autonomous driving. In *2021 IEEE Intelligent Vehicles Symposium (IV)*, pages 231–237. IEEE, 2021.
- [26] Mehdi Zemni, Mickaël Chen, Éloi Zablocki, Hédi Ben-Younes, Patrick Pérez, and Matthieu Cord. Octet: Object-aware counterfactual explanations. In *Proceedings of the IEEE/CVF Conference on Computer Vision and Pattern Recognition*, pages 15062–15071, 2023.
- [27] Gwangbin Kim, Dohyeon Yeo, Taewoo Jo, Daniela Rus, and SeungJun Kim. What and when to explain? on-road evaluation of explanations in highly automated vehicles. *Proceedings of the ACM on Interactive, Mobile, Wearable and Ubiquitous Technologies*, 7(3):1–26, 2023.
- [28] Tobias Schneider, Joana Hois, Alischa Rosenstein, Sandra Metzl, Ansgar RS Gerlicher, Sabiha Ghellal, and Steve Love. Don’t fail me! the level 5 autonomous driving information dilemma regarding transparency and user experience. In *Proceedings of the 28th International Conference on Intelligent User Interfaces*, pages 540–552, 2023.
- [29] Mert Yuksekgonul, Maggie Wang, and James Zou. Post-hoc concept bottleneck models. In *The Eleventh International Conference on Learning Representations*, 2023.
- [30] David B Leake. *Case-based reasoning: Experiences, lessons and future directions*. MIT press, 1996.
- [31] Mark T Keane and Eoin M Kenny. How case-based reasoning explains neural networks: A theoretical analysis of xai using post-hoc explanation-by-example from a survey of ann-cbr twin-systems. In *Case-Based Reasoning Research and Development: 27th International Conference, ICCBR 2019, Otzenhausen, Germany, September 8–12, 2019, Proceedings 27*, pages 155–171. Springer, 2019.
- [32] Frode Sørmo, Jörg Cassens, and Agnar Aamodt. Explanation in case-based reasoning—perspectives and goals. *Artificial Intelligence Review*, 24:109–143, 2005.
- [33] Roger C Schank. *Dynamic memory: A theory of reminding and learning in computers and people*. Cambridge University Press, 1983.
- [34] Napat Karnchanachari, Dimitris Geromichalos, Kok Seang Tan, Nanxiang Li, Christopher Eriksen, Shakiba Yaghoubi, Noushin Mehdipour, Gianmarco Bernasconi, Whye Kit Fong, Yiluan Guo, and Holger Caesar. Towards learning-based planning: The nuplan benchmark for real-world autonomous driving. In *2024 IEEE International Conference on Robotics and Automation (ICRA)*, pages 629–636, 2024.

- [35] Marc Heim, Francisco Suárez-Ruiz, Ishraq Bhuiyan, Bruno Brito, and Momchil S Tomov. Lab2car: A versatile wrapper for deploying experimental planners in complex real-world environments. In *2025 IEEE International Conference on Robotics and Automation (ICRA)*, pages 14828–14834. IEEE, 2025.
- [36] David Gunning and David Aha. Darpa’s explainable artificial intelligence (xai) program. *AI magazine*, 40(2):44–58, 2019.
- [37] Meadhbh I Foster and Mark T Keane. Surprise! you’ve got some explaining to do. In *Proceedings of the Annual Meeting of the Cognitive Science Society*, volume 35, 2013.
- [38] Robert R Hoffman, Shane T Mueller, Gary Klein, and Jordan Litman. Measures for explainable ai: Explanation goodness, user satisfaction, mental models, curiosity, trust, and human-ai performance. *Frontiers in Computer Science*, 5:1096257, 2023.
- [39] Gerd Gigerenzer and Ulrich Hoffrage. How to improve bayesian reasoning without instruction: frequency formats. *Psychological review*, 102(4):684, 1995.
- [40] Mica R Endsley. Measurement of situation awareness in dynamic systems. *Human factors*, 37(1):65–84, 1995.
- [41] Federal Aviation Administration. Flight test guide for certification of part 23 airplanes. Advisory Circular AC No. 23-8C, U.S. Department of Transportation, 11 2011. Initiated By: ACE-100.
- [42] Lindsay Sanneman and Julie A Shah. The situation awareness framework for explainable ai (safe-ai) and human factors considerations for xai systems. *International Journal of Human-Computer Interaction*, 38(18-20):1772–1788, 2022.
- [43] Eoin M Kenny, Courtney Ford, Molly Quinn, and Mark T Keane. Explaining black-box classifiers using post-hoc explanations-by-example: The effect of explanations and error-rates in xai user studies. *Artificial Intelligence*, 294:103459, 2021.

8 Methods

8.1 Architecture

The black-box ML planner uses a modified version of the DriveIRL architecture (Figure 1b) [1, 2]. For the trajectory generator G , we use a heuristic generator that produces 143 jerk-optimal trajectories to anchor waypoints along the route. For the scene encoder H , we use the hierarchical vector transformer (HiVT) [3] pretrained for multi-agent motion prediction. In addition to the scene embedding \mathbf{h} , this produces an additional 3 trajectories for the AV, for a total of $k = 146$ candidate trajectories. In the scene-trajectory encoder E , trajectories are encoded using a recurrent neural network (RNN) and then fed jointly with the scene embedding into a transformer layer which produces the scene-trajectory embeddings \mathbf{z}_i . The reward model R is a multi-layer perceptron (MLP). In CW-Net (Figure 1c), the classifier C and the new reward model R' are MLPs.

We avoided testing other methods besides CW-Net because, at the time of writing, we are unaware of other works which are capable of modeling interpretable-by-design IRL systems, and we seek the most general comparison possible of concept-based explanations against no explanation.

8.2 CW-Net training

We used two datasets:

- Dataset 1: 500,000 scenarios, 8 concept labels (Table S2), and
- Dataset 2: 3,000,000 scenarios, 10 concept labels (Table S3).

For a full list of the concept labels and their meanings, see Section 8.5. Each scenario was associated with 146 trajectories, thus giving between 70.5-423 million training data points for the concept classifier, each with multiple concept labels. Our algorithm assumes CW-Net training has access to the original dataset used to train the black-box ML planner, along with annotated human-understandable concept labels for each of these data points. The annotations can be multi-label, meaning that one datum can be associated with as many concepts as desired or useful. The experiments with CLOSE and ASV concepts used models trained on Dataset 1. The experiments with BIKE and PEDESTRIAN concepts used models trained on Dataset 2.

During training, the parameters of the trajectory generator G , the scene encoder H , and the scene-trajectory encoder E are frozen, and only the concept classifier C and the new reward model R' are trainable. Two separate losses are optimized simultaneously.

First, a concept classification loss $\mathcal{L}_{\text{concept}}$ is used to train C to predict the correct concept label(s). In our setting, this loss combines cross-entropy with binary cross-entropy for different concepts, depending on the semantics of the corresponding scenario types. For example, in Dataset 1, we use cross-entropy to model the steering concepts of the car (LEFT, RIGHT, and STRAIGHT), and the speed concepts (STOPPED, SLOW), while also using binary cross-entropy to predict the presence of other concepts

such as **ASV**, **INTERSECTION**, and **CLOSE**. These losses are then averaged into one:

$$\mathcal{L}_{\text{concept}} = \frac{1}{2k} \sum_{i=1}^k \left(\frac{1}{M_{\text{CCE}}} \sum_{j=1}^{M_{\text{CCE}}} \mathcal{L}_{\text{CCE}}(c_{i,j}, \hat{c}_{i,j}) + \frac{1}{M_{\text{BCE}}} \sum_{l=1}^{M_{\text{BCE}}} \mathcal{L}_{\text{BCE}}(c_{i,l}, \hat{c}_{i,l}) \right)$$

where M_{CCE} is the number of concepts modeled using categorical cross-entropy (e.g., steering and speed), and M_{BCE} is the number of concepts modeled using binary cross-entropy (e.g., presence of features like **ASV**, **INTERSECTION**, and **CLOSE**). $c_{i,j}$ and $\hat{c}_{i,j}$ represent the true and predicted labels for the j -th concept under CCE for the i -th data point, while $c_{i,l}$ and $\hat{c}_{i,l}$ represent the true and predicted labels for the l -th concept under BCE for the i -th data point. On Dataset 2, we take a different approach and model everything, including the speed concepts (**STOPPED**, **SLOW**, and **FAST**), with binary cross-entropy. In general, these parameters can be tuned to fit the task at hand.

Secondly, a cross-entropy loss $\mathcal{L}_{\text{trajectory}}$ is used to train the network to predict the correct trajectory, which we define as the original trajectory chosen by the black-box planner. Both losses are averaged:

$$\mathcal{L}_{\text{total}} = \frac{1}{2} (\mathcal{L}_{\text{concept}} + \mathcal{L}_{\text{trajectory}})$$

A focal loss [4] is applied to counteract data imbalances, just as in the original DriveIRL planner [1, 2]. Computationally, our networks were trained on a large distributed setup using PyTorch Lightning.

8.3 Concept separation

When adding interpretability modules post hoc, as we have, there is the possibility that the network will not have learned to separate the concepts of interest, and thus fail to be able to predict them accurately [5]. In fact, we observed this in Motional’s experimental prototype which we tested (see Table S3), when certain concepts such as **CLOSE** and **PEDESTRIAN** had poor precision and high recall, relatively speaking. There are two important points to note here. First, the better trained and more sophisticated an architecture is, the more it naturally learns to separate an impressive number of concepts in an unsupervised manner [6, 7] (often in the millions), so this is unlikely to be an issue for most companies with the flagship models in the future. Secondly, even if CW-Net has not learned to separate certain concepts (e.g., red traffic lights vs. green ones), this could highlight the reason why the AV fails to act appropriately (e.g., stop vs. go) a given situation (e.g., because there are insufficient traffic light scenarios in the training data). Hence, from an explainability point of view, even concepts with low accuracy can be useful, as we demonstrate in the paper.

8.4 Alternative architecture

Alongside our primary causal architecture illustrated in Figure 1, we also developed an alternative which gave post-hoc justifications for AV behavior (Figure S1). Specifically, we froze the weights of the pretrained black-box ML planner and trained a

concept classifier head C to work in parallel to the reward layer R . Similarly to the causal architecture (Fig 1c), C used the scene-trajectory embeddings \mathbf{z}_i to classify the concepts. This approach is beneficial because of its relative simplicity and accessibility, although the drawback is that it may be less faithful to the model’s reasoning process, as the concept classifications are not directly used by the model to rank state-trajectory pairs. However, there is ample evidence that such explanations are often faithful and capable [8, 9], so we include both as an option and demonstrate the utility of both. Specifically, this parallel architecture was used in the real-world scenarios with the CLOSE concept (Section 5.1).

8.5 Concept details

Dataset 1 concepts were as follows:

- **LEFT, RIGHT, STRAIGHT**: Classification of driving direction concepts, trained with cross-entropy loss. For example, the concept **LEFT** represents training scenarios where the car was turning left.
- **STOPPED, SLOW**: Classification of car speed concepts, trained with cross-entropy loss. The concept of e.g. **STOPPED** represents training scenarios where the car was stopped.
- **ASV** (approaching stopped vehicle): Scenarios in which the car was approaching stopped a vehicle. Trained with binary cross-entropy.
- **INTERSECTION**: Scenarios in which the car was at an intersection. Trained with binary cross-entropy.
- **CLOSE**: Scenarios in which the car was within 3 meters of another vehicle. Trained with binary cross-entropy.

Dataset 2 had the following concepts:

- **SLOW**: Scenarios in which the car was driving at 1-2 m/s.
- **STOPPED**: Scenarios in which the car was stationary.
- **FAST**: Scenarios in which the car was driving faster than 2 m/s.
- **STOP SIGN**: Scenarios in which the car was close to a stop sign.
- **TRAFFIC LIGHT**: Scenarios in which the car was close to a traffic light.
- **INTERSECTION**: Scenarios in which the car was at an intersection.
- **Pedestrian**: Scenarios in which the car was close to a pedestrian.
- **FOLLOWING**: Scenarios in which the car was following another vehicle.
- **BIKE**: Scenarios in which the car was close to a cyclist.
- **PUDO** (pedestrian pickup/drop-off): Scenarios in which the car was in a pedestrian pickup/drop-off zone.

All concepts in Dataset 2 were trained with a binary cross-entropy loss.

Although the AV was trained on 8-12 concepts (depending on the dataset), we focus our study on a subset of concepts (**CLOSE**, **ASV**, **BIKE**, **PEDESTRIAN**) because they are the only ones which relate to other road users and are easy to test counterfactually. The concept **FOLLOWS** involves other road users too, but no notable occurrences happened during real-world deployment.

Simulation results

We tested our CW-Net model across the entire nuPlan validation dataset to see how its driving performance compares to the original black-box ML planner it was trained from. The dataset represents the world’s first large-scale planning benchmark for autonomous driving [10] and measures how close a trained AV is to a human expert in L_2 distance, progress along the route, and safety (no collisions). In the black-box model, when following the lane or decelerating from high speed, the planner was able to make progress along the route ($> 93\%$ of human driving distance), while avoiding collisions ($> 90\%$ collision-free) and staying close to the ground-truth human expert trajectory (< 1 m displacement at 5 s). Performance was worse when starting from a stop, with less progress (74% of human driving distance), more collisions (81% collision-free), and greater deviation from the human expert (1.2 m displacement at 5 s). Overall, the results showed our variation of the AV architecture had less than 0.01 L_2 difference to the original black-box agent on average across all measurements, and not meaningfully different, showing that it is possible to train our more interpretable model in Figure 1 without sacrificing performance. The full results are in Table S1.

For concept accuracy verification, we used 5% holdout data from our training datasets, the results are given in Table S2 and Table S3. Across both datasets, the mean accuracy was 0.54, precision 0.23, recall 0.77, and F1 Score 0.31. Overall, the results suggested that CW-Net did not separate all concepts equally well, which suits our purposes as the explanations will highlight when and how this happens, and how it relates to driving performance, thus helping with mental model refinement (see Section 8.3). Notable results include an F1 score of 0.82 for detecting the SLOW concept, and < 0.00 for detecting the BIKE concept, showing the latter is perhaps not well encoded or understood by the car.

Mental model elicitation studies

These studies were designed to replicate the driver’s experiences in the private track tests (Section 5) with a larger cohort, in order to help demonstrate the robustness of our findings regarding the drivers’ mental models (Figure S2). The same study was run separately with experts (other drivers and test engineers from Motional) and non-experts (randomly sampled users from Prolific.com). Specifically, we were interested in testing the following hypotheses:

- Hypothesis 1: The participants’ responses *before* observing the explanation (in the video replay) would be more consistent with the belief of the safety driver *before* observing the explanation (in the car).
- Hypothesis 2: The participants’ responses *after* observing the explanation would be more consistent with the belief of the safety driver *after* observing the explanation.
- Hypothesis 3: The participants’ responses *after* observing the explanation would be more consistent with the ground-truth reason for AV behavior.
- Hypothesis 4: Counterfactual prediction ability would correlate with user mental model goodness, the latter as measured by the nearest-neighbor tasks and the free-form text response of Hoffman et al. [11].

- Hypothesis 5: The two measures of mental model goodness would correlate with each other and have similar distributions across groups.

Design and Materials

We focused on the same three surprising events observed during the private track tests. The experiment was designed to measure mental models through a combination of nearest-neighbor and prediction tasks, accompanied by confidence scores and free-form text responses, in which we could probe the participants’ mental models [11] (Figure S3). First, users saw the respective video, and were asked to rate two possible reasons for AV behaviour, along with confidence scores (i.e., the nearest-neighbor mental model elicitation task). Then, users were asked to make the same counterfactual prediction as the driver (i.e., the prediction task), along with a confidence score, and a free-form text rationale explaining their reasoning. Then, users saw the same video with the explanation, and repeated the questions. This within-subject design mirrors the experience of the safety drivers during the on-road tests.

Subjects

For the expert group, we recruited 9 safety drivers, test engineers, and test specialists from Motional (aged between 18-80, 8 male and 1 female). All participants volunteered to participate and were not paid. For non-experts we sampled users sourced from Prolific.com, which is known for its high-quality user base. Thirty users were randomly sampled U.S. citizens aged between 18-80, native English speakers, and an even number of male/female. To ensure high-quality text responses, we paid users above the average rate with 15 USD per hour and stressed that they should only take the study if they were certain they understood the instructions.

Metrics

We used the nearest-neighbor task and the free-form text rationale as direct measures of mental models. For the nearest-neighbor task, we measured mental model goodness as a combination of choice accuracy and confidence. Specifically, we formalized mental model improvement as shifting from an incorrect to a correct belief (w.r.t. the ground-truth reasons for AV behavior), or increasing confidence in the correct belief, or decreasing confidence in the incorrect belief (Figure S4). For the free-form text rationale, we employed an LLM-as-a-judge (GPT-5) to determine which text response (before or after observing the CW-Net explanation) is closer to the ground-truth reason for AV behavior. The LLM prompts were tuned over 3 iterations on the expert responses (Figure S6) and then evaluated once on the non-expert responses (Figure S7). Mental model improvement was formalized as instances where the free-form response after observing the CW-Net explanation is closer to the ground truth, compared to the free-form response before observing the explanation.

We used the prediction task as a measure of downstream performance that relies on mental models, thus measuring them indirectly [12, 13]. We measured prediction improvement as a combination of choice accuracy and confidence in the same way as for the nearest-neighbor task (Figure S5).

To analyze the relationship between direct (nearest neighbor, free-form text rational) and indirect (prediction) measures of mental models, we employed a Linear Mixed-Effects Model (LME) to evaluate the effect of the mental model change (improve/worsened) on the prediction change variable (i.e., the delta in confidence change in the prediction), while controlling for individual participant variation as a random effect (Figure S9). To collapse accuracy/confidence on a single scale for computing the confidence deltas, we simply flipped the sign of confidence values for inaccurate beliefs to negative. All code for this analysis is available (see code availability below).

Results

We found evidence favoring all of our hypotheses.

- Hypothesis 1: The participants' *initial* belief (before observing the explanation) was often times more similar to the safety driver's *initial* belief ($p < 10^{-9}$, exact binomial test).
- Hypothesis 2: The participants' *final* belief (after observing the explanation) was often times more similar to the safety driver's *final* belief ($p < 0.0002$, exact binomial test).
- Hypothesis 3: The participants' *final* belief (after observing the explanation) was often times more similar to the ground truth ($p < 10^{-5}$, exact binomial test).
- Hypothesis 4: There was a clear relationship between mental model category and predictive ability of users, with only nearest neighbor categories failing to reach significance with experts (see Figure S9).
- Hypothesis 5: Interaction analysis revealed no significant difference in the relationship between nearest-neighbor score improvement and text rationale improvement across the two groups ($p = 0.842$; Figure S8), indicating a consistent underlying mechanism for both experts and non-experts. Non-experts demonstrated a significant positive correlation ($\beta = 0.27, p < 0.001$), suggesting that improved scores were strong predictors of improved mental model rationale in this group. While experts exhibited a nearly identical positive coefficient ($\beta = 0.23$), the relationship did not reach statistical significance, likely due to a smaller sample ($p = 0.243$).

Public roads evaluation using SAGAT

We deployed CW-Net in manual mode on Las Vegas public roads to collect complex, naturalistic scenarios analogous to those already discovered during the private track tests (Figure S10). We used these as materials for an online Situation Awareness Global Assessment Technique (SAGAT) study ($N = 100$). This setup allows us to validate the robustness of the CW-Net explanations using a well-established rigorous framework (Figure S2). We used a between-subject design in which we compared CW-Net explanations (experimental group) against baseline explanations describing speed and steering (control group) [14] (Figure S11).

Gathering materials

We collected data for ASV (01:02:55), CLOSE (00:50:42), and BIKE (>3 hours). We labeled sequences where human driving mimicked the ML planner in surprising scenarios that resembled those already discovered in the private track tests (e.g., CLOSE: stuck beside vehicles; ASV: braking for hallucinations; Figure S10). PEDESTRIAN replaced BIKE due to there being no naturally occurring cyclists in the new video data. We sampled two surprising events per concept (6 total) and six corresponding “unsurprising” events to ensure explanations did not degrade situational awareness in regular driving (Table S6). Activation thresholds were 0.5 for ASV/PEDESTRIAN and 0.94 for CLOSE, derived from prior private track data (Figure 3).

Note the distribution of concept activations did not change significantly between the private-track tests and the public-road tests (Table S8), despite the tests being performed more than a year apart, on different AV’s, with different software stacks, and under completely different conditions. This demonstrates the robustness and reliability of the algorithm.

Study design

We used a between-subjects design (N=100) assessing SAGAT perception, comprehension, and projection. Participants were split into experimental (CW-Net explanations) and control (speed/steering placeholder) groups. Attention checks based on material content and viewing times excluded 4 participants, leaving 48 per group.

Materials

Stimuli included 13 videos (6 surprising, 6 unsurprising, 1 attention check). The experimental group saw concept activations, while the control saw speed and steering data (Figure S12, S13, S14). Following each video, a “blackout” screen presented six binary questions: four related to *perception*, one to *comprehension*, and one to *projection*.

Subjects

We recruited gender-balanced U.S. residents (18+, native English speakers) via Prolific.com. Subjects were paid \$12/hr. The study received MIT IRB approval.

Metrics

We analyzed the average average of each participant on each question type using two-tailed t-tests, splitting data by surprising vs. unsurprising events for each situational awareness dimension.

Results

Results are displayed in Figure S15. In surprising events, explanations significantly improved situational awareness after Bonferroni correction, showing large effect sizes for perception (Cohen’s $d = 1.290$) and comprehension ($d = 0.996$), and a medium effect for projection ($d = 0.606$). In unsurprising events, no significant differences occurred (perception $d = 0.085$, projection $d = -0.142$, comprehension $d = -0.514$), confirming that explanations provided benefit in anomalous situations

without adversely affecting situational awareness during routine operations. Additionally, we confirmed feature robustness by comparing concept distributions to prior private track tests using Wasserstein distance (Table S8), finding no meaningful changes.

8.6 Data availability

The data used for plotting in the paper’s figures is available at https://drive.google.com/drive/folders/1Lz6OGGi2gFeBOnC3ddyZFJMztqUTC_Am?usp=sharing. The user study data are also available at the same address. The concept classification and ranker classification data is not available, along with the model weights, videos, and nuPlan results, due to data privacy and intellectual property issues. However, any person may reproduce similar results by training their own model on the nuPlan dataset available online, and following the instructions in the paper, although they will need to label the data with concepts of interest. Motional and MIT are happy to assist any research effort to do this. We have also provided a code capsule which reproduces the results in another domain.

8.7 Code availability

CW-Net code for the models used is available at https://drive.google.com/drive/folders/1Lz6OGGi2gFeBOnC3ddyZFJMztqUTC_Am?usp=sharing. Due to Motional intellectual property issues, the code for training the AV used in the paper cannot be made available. However, code to implement and train CW-Net architectures will be available at https://github.com/EoinKenny/CW_Net, which can be used to train an interpretable agent in any domain as long as concept labels are present, this will help reproduce similar results in any domain. The full user survey will also be available to reproduce the user study in the same repo, but without the videos. Lastly, the code to implement our LLM-as-a-judge for the mental model analysis is available at <https://github.com/tomov/xai-sdc-mit-motional-survey-responses/tree/main>.

Acknowledgements

We thank Tom Bewley of JPMC AI research, Mycal Tucker of Anthropic, and Winthrop Gillis of Harvard for reviewing an early version of the manuscript.

Author contributions

E.M.K contributed to conceptualization of the research, model training, experimental evaluation, writing. A.D., S.U.L., T.P.M., S.R., Y.H., and M.S.T. all contributed to the technical implementation of the algorithm in the self-driving car. L.M. contributed to project organization, and writing. M.S.T. and J.A.S. contributed to conceptualization of the research, project organization, and writing.

Competing interests

The authors declare no competing interests.

Additional information

Supplementary information available at https://drive.google.com/drive/folders/1Lz6OGGi2gFeBOnC3ddyZFJMztqUTC_Am?usp=sharing and https://github.com/EoinKenny/CW_Net. Correspondence and requests for materials should be addressed to Eoin M. Kenny.

References

- [1] Momchil S. Tomov, Sang Uk Lee, Hansford Hendrigo, Jinwook Huh, Teawon Han, Forbes Howington, Rafael da Silva, Gianmarco Bernasconi, Marc Heim, Samuel Findler, Xiaonan Ji, Alexander Boule, Michael Napoli, Kuo Chen, Jesse Miller, Boaz Floor, and Yunqing Hu. Treeirl: Safe urban driving with tree search and inverse reinforcement learning. 2025.
- [2] Tung Phan-Minh, Forbes Howington, Ting-Sheng Chu, Momchil S Tomov, Robert E Beaudoin, Sang Uk Lee, Nanxiang Li, Caglayan Dicle, Samuel Findler, Francisco Suarez-Ruiz, et al. Driveirl: Drive in real life with inverse reinforcement learning. In *2023 IEEE International Conference on Robotics and Automation (ICRA)*, pages 1544–1550. IEEE, 2023.
- [3] Zikang Zhou, Luyao Ye, Jianping Wang, Kui Wu, and Kejie Lu. Hivt: Hierarchical vector transformer for multi-agent motion prediction. In *Proceedings of the IEEE/CVF Conference on Computer Vision and Pattern Recognition*, pages 8823–8833, 2022.
- [4] Tsung-Yi Lin, Priya Goyal, Ross Girshick, Kaiming He, and Piotr Dollár. Focal loss for dense object detection. In *Proceedings of the IEEE international conference on computer vision*, pages 2980–2988, 2017.
- [5] Simon Schrodi, Julian Schur, Max Argus, and Thomas Brox. Concept bottleneck models without predefined concepts. *arXiv preprint arXiv:2407.03921*, 2024.
- [6] Adly Templeton, Tom Conerly, Jonathan Marcus, Jack Lindsey, Trenton Bricken, Brian Chen, Adam Pearce, Craig Citro, Emmanuel Ameisen, Andy Jones, Hoagy Cunningham, Nicholas L Turner, Callum McDougall, Monte MacDiarmid, C. Daniel Freeman, Theodore R. Sumers, Edward Rees, Joshua Batson, Adam Jermyn, Shan Carter, Chris Olah, and Tom Henighan. Scaling monosemanticity: Extracting interpretable features from claude 3 sonnet. *Transformer Circuits Thread*, 2024.
- [7] Christopher D Manning, Kevin Clark, John Hewitt, Urvashi Khandelwal, and Omer Levy. Emergent linguistic structure in artificial neural networks trained by self-supervision. *Proceedings of the National Academy of Sciences*, 117(48):30046–30054, 2020.

- [8] Marco Tullio Ribeiro, Sameer Singh, and Carlos Guestrin. ” why should i trust you?” explaining the predictions of any classifier. In *Proceedings of the 22nd ACM SIGKDD international conference on knowledge discovery and data mining*, pages 1135–1144, 2016.
- [9] M Scott, Lee Su-In, et al. A unified approach to interpreting model predictions. *Advances in neural information processing systems*, 30:4765–4774, 2017.
- [10] Napat Karnchanachari, Dimitris Geromichalos, Kok Seang Tan, Nanxiang Li, Christopher Eriksen, Shakiba Yaghoubi, Noushin Mehdipour, Gianmarco Bernasconi, Whye Kit Fong, Yiluan Guo, and Holger Caesar. Towards learning-based planning: The nuPlan benchmark for real-world autonomous driving. In *2024 IEEE International Conference on Robotics and Automation (ICRA)*, pages 629–636, 2024.
- [11] Robert R Hoffman, Shane T Mueller, Gary Klein, and Jordan Litman. Measures for explainable ai: Explanation goodness, user satisfaction, mental models, curiosity, trust, and human-ai performance. *Frontiers in Computer Science*, 5:1096257, 2023.
- [12] Mica R Endsley. Measurement of situation awareness in dynamic systems. *Human factors*, 37(1):65–84, 1995.
- [13] Mica R Endsley. Direct measurement of situation awareness: Validity and use of sagat. In *Situational awareness*, pages 129–156. Routledge, 2017.
- [14] Eoin M Kenny, Courtney Ford, Molly Quinn, and Mark T Keane. Explaining black-box classifiers using post-hoc explanations-by-example: The effect of explanations and error-rates in xai user studies. *Artificial Intelligence*, 294:103459, 2021.

Supplementary Material

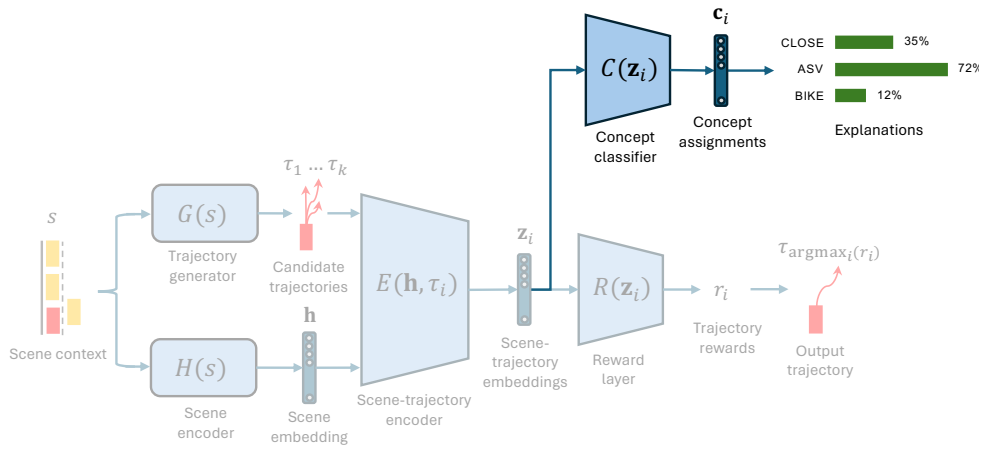


Fig. S1 Parallel architecture: This is identical to the black-box planner (Figure 1b; greyed out here), except the scene-trajectory embeddings are fed to the concept classifier C in parallel to the (original) reward model R . The black-box part of the architecture (greyed out) is kept frozen. These concept classifications are then converted to probabilities (x100 to convert to percentages) and presented to the user.

Scenario type	Metric	CW-Net	ML planner
Nominal lane follow (968 scenarios)	Average L2 error	4.202058	4.200189
	Average L2 error 3s	0.401251	0.400440
	Average L2 error 5s	0.780286	0.778495
	Average L2 error 10s	2.141165	2.136004
	Progress along expert route	0.939595	0.939382
	No at fault collisions	0.909091	0.909091
Decelerating from high speed (1099 scenarios)	Average L2 error	3.139028	3.144618
	Average L2 error 3s	0.533925	0.533905
	Average L2 error 5s	0.930384	0.929786
	Average L2 error 10s	2.056039	2.053457
	Progress along expert route	0.990187	0.990213
	No at fault collisions	0.945405	0.942675
	Deceleration time difference	0.443201	0.439381
Start accelerating from stationary (919 scenarios)	Average L2 error	8.919248	9.019697
	Average L2 error 3s	0.426693	0.425365
	Average L2 error 5s	1.244357	1.249598
	Average L2 error 10s	4.611888	4.673006
	Progress along expert route	0.740881	0.736437
	No at fault collisions	0.807399	0.803047
	Start from stationary max speed difference	0.239367	0.241552
	Start from stationary time delay	3.477263	3.494675

Table S1 Full nuPlan results comparing driving performance of our CW-Net planner to the original black-box ML planner.

	Accuracy	Precision	Recall	F1 Score
Steering	0.62		(cross entropy)	
Speed	0.83		(cross entropy)	
Approaching stopped vehicle (ASV)	0.55	0.20	0.89	0.33
Intersection	0.51	0.42	0.61	0.49
CLOSE to another vehicle	0.45	0.10	0.81	0.17
Ranker accuracy	0.94			

Table S2 CW-Net concept classification performance on Dataset 1

	Accuracy	Precision	Recall	F1 Score
Slow	0.83	0.73	0.93	0.82
Stopped	0.48	0.16	0.81	0.27
Fast	0.68	0.49	0.86	0.63
Stop sign	0.43	0.03	0.84	0.05
Traffic light	0.39	0.16	0.62	0.25
Intersection	0.42	0.20	0.65	0.31
Pedestrian	0.44	0.03	0.84	0.07
Following	0.43	0.02	0.84	0.04
BIKE	0.21	0.00	0.42	0.00
PUDO	0.58	0.30	0.86	0.44
Ranker accuracy	0.95			

Table S3 CW-Net concept classification performance on Dataset 2.

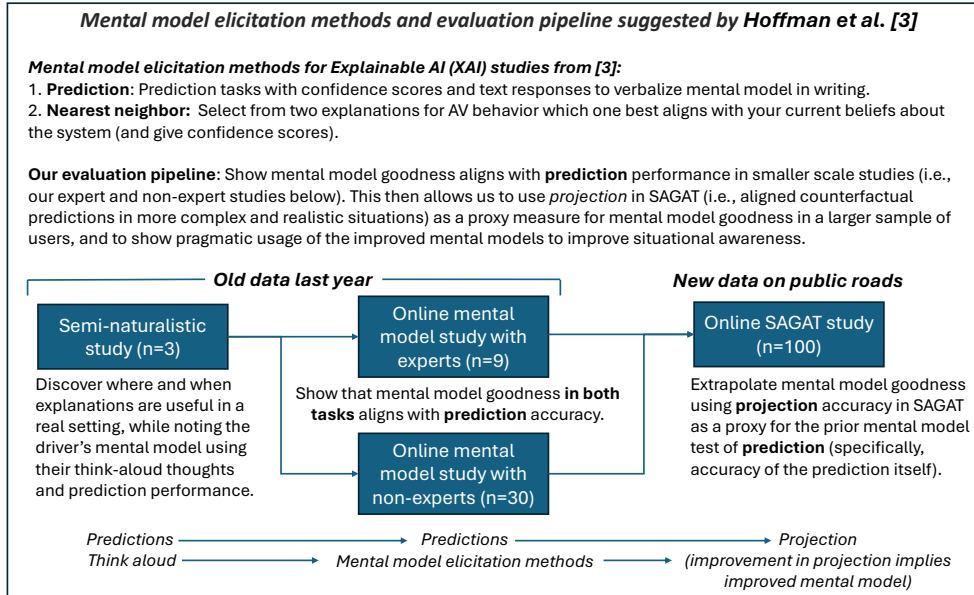


Fig. S2 Study methodology. First we collected a series of surprising situations expert safety drivers encountered during their day-to-day job testing the AV where the explanations proved to be useful to understand why the AV made certain decisions and how it would behave in alternative scenarios. During these situations, we noted the driver’s mental model through their think-aloud thoughts and behaviour. A mental model elicitation study was run with more expert drivers and non-experts online to more robustly verify these findings and if mental model goodness did indeed correlate with counterfactual predictive performance. Then, in a large-scale SAGAT study, we used *projection* as a surrogate metric for mental model quality, since it perfectly matches the prior prediction tasks.

Scenario/concept	Before explanation	After explanation
CLOSE	0.00%	11.11%
ASV	33.33%	44.44%
BIKE	77.78%	77.78%
Overall average	37.04%	44.44%

Table S4 Performance improvement on prediction task ($N = 9$ experts).

Scenario/concept	Before explanation	After explanation
CLOSE	3.33%	33.33%
ASV	36.67%	60.00%
BIKE	40.00%	66.67%
Overall average	26.67%	53.33%

Table S5 Performance improvement on prediction task ($N = 30$ non-experts).

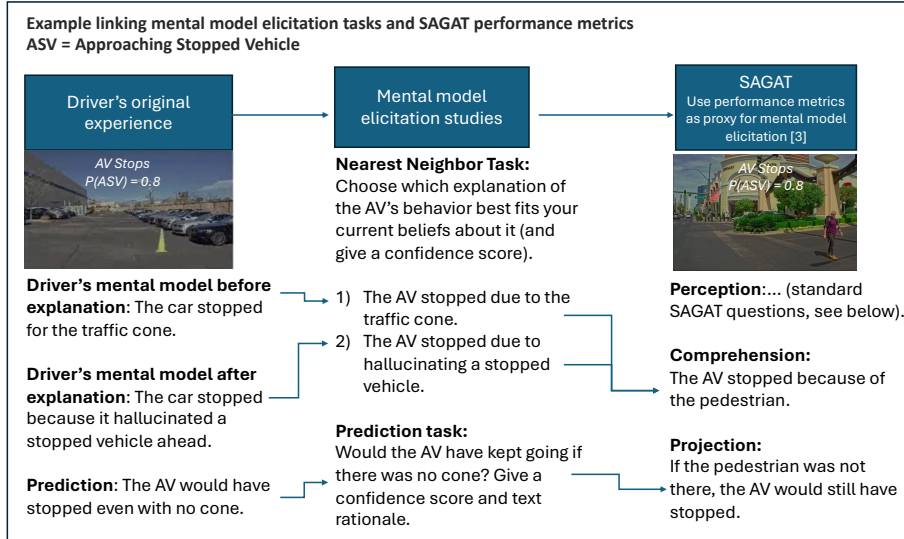


Fig. S3 Study pipeline example. We noted the safety drivers' think-aloud thoughts and predictions in surprising situations encountered during the on-road tests. In the subsequent online mental model elicitation study, we used their beliefs about AV behaviour before/after the explanation in the nearest-neighbor task and their predictions about future AV future behavior in the prediction task. The nearest-neighbor task resembles the comprehension task in the follow-up SAGAT study. The prediction task corresponds exactly to the projection task in the SAGAT study.

Testing concept robustness			
Concept activation	AV speed	Concept accuracy	
<i>Original</i>			
ASV	High	Brakes	Bad
CLOSE	High	Frozen	Good
BIKE	Low	Moving	Low
<i>Modified for robustness</i>			
ASV	High	Brakes	Good
CLOSE	Low	Frozen	Good
BIKE	Low	Stopped	Low

Table S6 Selecting unsurprising events for SAGAT study. To select unsurprising events we modified what was individual unusual about each surprising event which fell into three categories. ASV: This concept was surprising because of the misclassification of the concept, so we selected a scenario in which it accurately classified the concept. CLOSE: This was surprising because the concept activation was higher than usual while the AV stopped, so we chose scenarios in which the AV stopped, but the concept activation was closer to its mean value. BIKE: This was unusual because the AV stopped seemingly due to the cyclist, so we chose scenarios in which the AV again stopped for other reasons. In all three setups, we only altered the one respective dimension, the other two remained static.

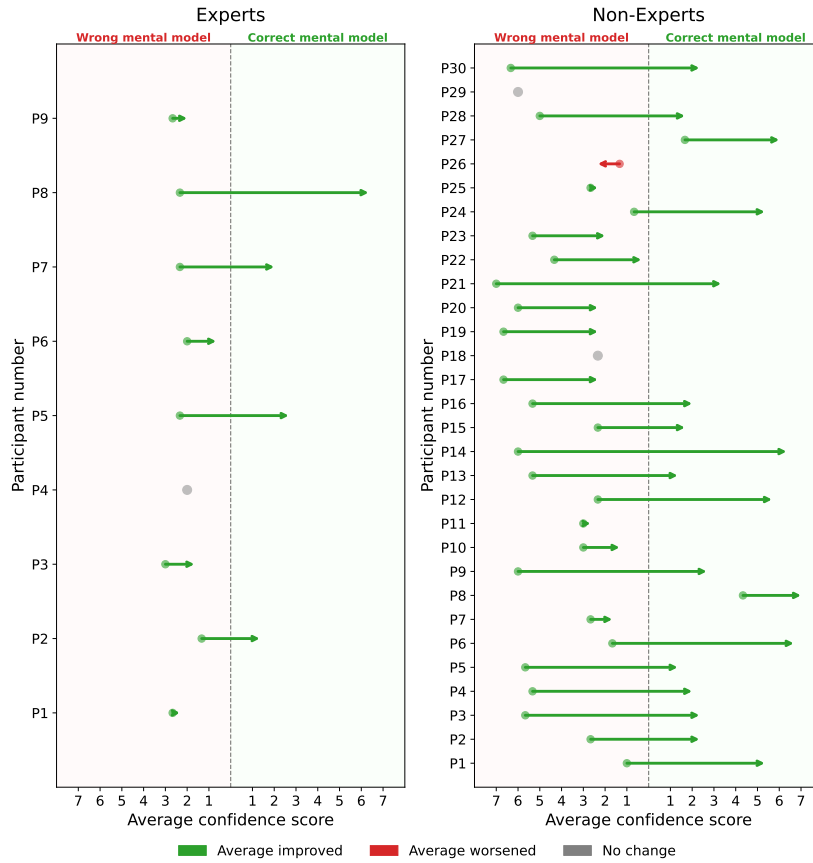


Fig. S4 Mental model improvement on nearest-neighbor task. Visualizing belief updates in response to the explanations for experts (left) and non-experts (right) on the nearest-neighbor task. Arrows originate at the participants' initial accuracy/confidence (before observing the explanation) and terminate at their final accuracy/confidence (after observing the explanation). For each participant, initial and final accuracy/confidence is averaged across all 3 scenarios. Green arrows indicate improvement in choice accuracy/confidence, while red arrows indicate worsening. Gray points represent participants with no change in beliefs.

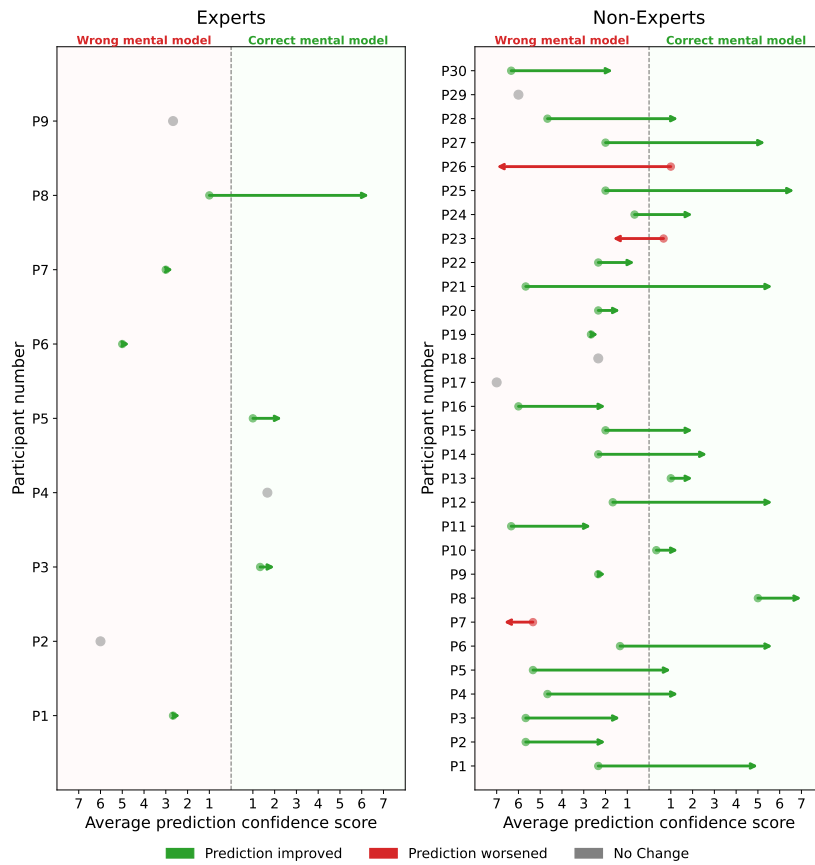


Fig. S5 Performance improvement on prediction task. Visualizing belief updates in response to the explanations for experts (left) and non-experts (right) on the prediction task. Notation as in Figure S4.

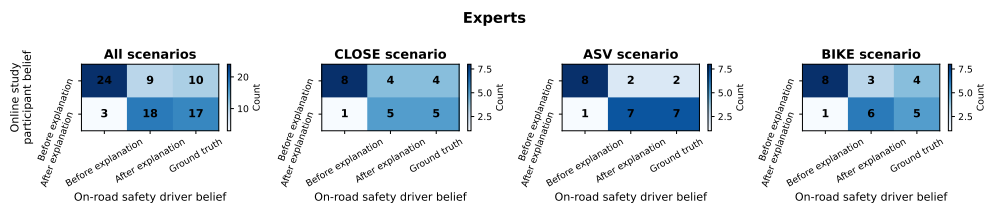


Fig. S6 Mental model improvement on free-form text rationale ($N = 9$ experts). Confusion matrices with participant beliefs (mental model and predictions) extracted from free-form responses in the mental model elicitation study study (y-axis) compared to beliefs from the safety drivers from the on-road tests and the ground truth explanation for AV behavior (x-axis). Numbers indicate raw response counts.

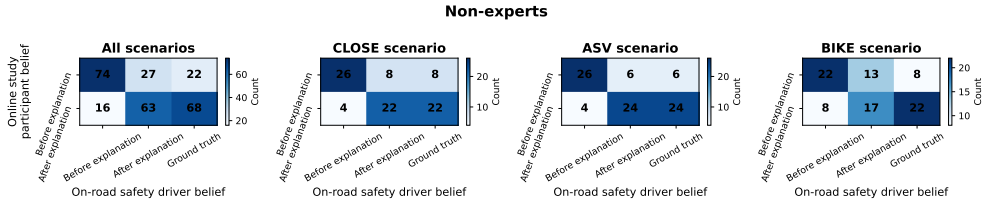


Fig. S7 Mental model improvement on free-form text rationale ($N = 30$ non-experts). Notation as in Figure S6.

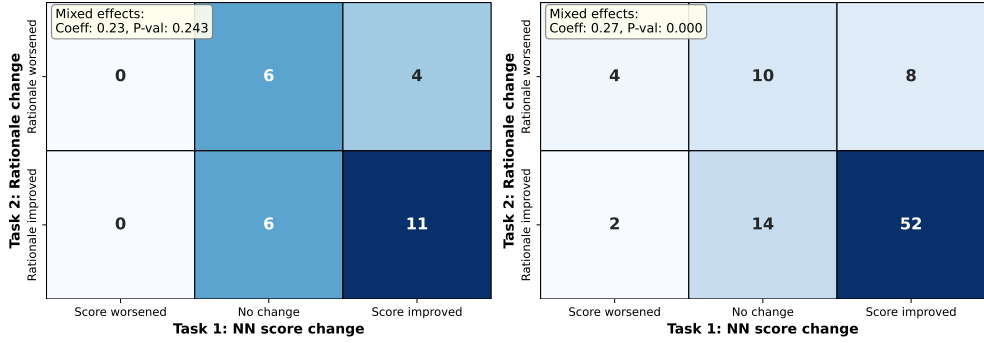


Fig. S8 Correlation between mental model metrics across groups. Heatmaps displaying the frequency of alignment between changes in nearest-neighbor (NN) task responses and the free-form text rationale. To determine if the relationship between these two mental model proxies differs by expertise, we performed ordinary least-squares (OLS) regression with clustered standard errors, including an interaction term. The interaction between group (experts vs. non-experts) and score change was not significant ($\beta = 0.04$, $p = 0.842$), indicating that the relationship between quantitative score improvements and qualitative rationale improvements is largely consistent across both groups.

Valence	Dimension	Effect direction	Cohen's d	p -value	Bonferroni significant
Surprising events	Perception	Exp > Control	1.290 (large)	< 0.001	Yes
	Comprehension	Exp > Control	0.996 (large)	< 0.001	Yes
	Projection	Exp > Control	0.606 (medium)	0.003	Yes
Unsurprising events	Perception	No effect	0.085 (negligible)	0.667	No
	Comprehension	Control > Exp	-0.514 (medium)	0.011	No
	Projection	No effect	-0.142 (negligible)	0.481	No

Table S7 SAGAT study results. During the ‘surprising’ events, explanations had an all-around positive impact on people’s situational awareness and thus their mental models. Conversely, during ‘unsurprising’ events, there were no significant differences between groups, after Bonferroni correction.

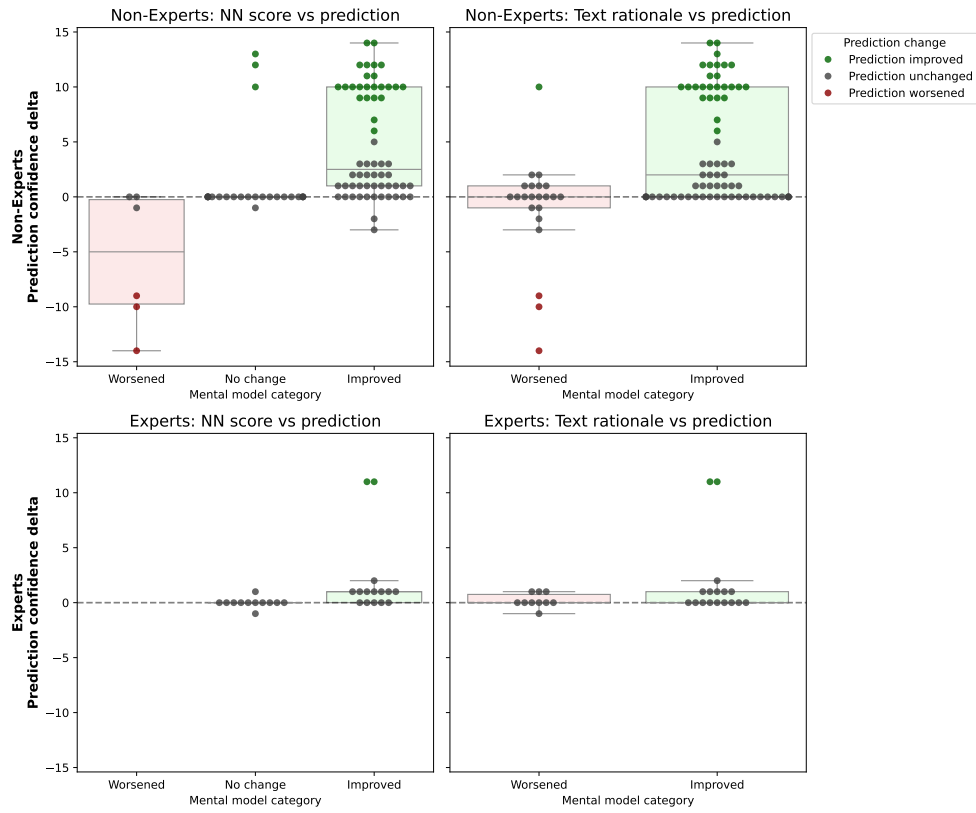


Fig. S9 Mental model improvement correlates with prediction improvement. Linear mixed effects (LME) models were used to analyze the relationship between changes in mental model proxies (nearest-neighbor task and free-form text rationale) and prediction accuracy/confidence. Specifically, the y-axis indicates each participant's Likert confidence after explanation minus before, positive scores indicate they moved towards the correct prediction, and green dots indicate the prediction flipped correctly. For experts ($N = 9$ participants \times 3 scenarios), improvement in the nearest-neighbor (NN) task significantly correlates with prediction improvement ($\beta = 2.02, SE = 0.87, p = 0.02$). The text rationale shows a similar positive effect ($\beta = 1.70, SE = 0.91, p = 0.06$), although it does not reach significance. For non-experts ($N = 30$ participants \times 3 scenarios), both NN improvement ($\beta = 9.86, SE = 2.07, p < 0.001$) and text rationale improvement ($\beta = 5.03, SE = 1.23, p < 0.001$) are significantly correlated with prediction improvement. Positive betas indicate that improving the mental model proxy is associated with a higher increase in prediction accuracy/confidence.

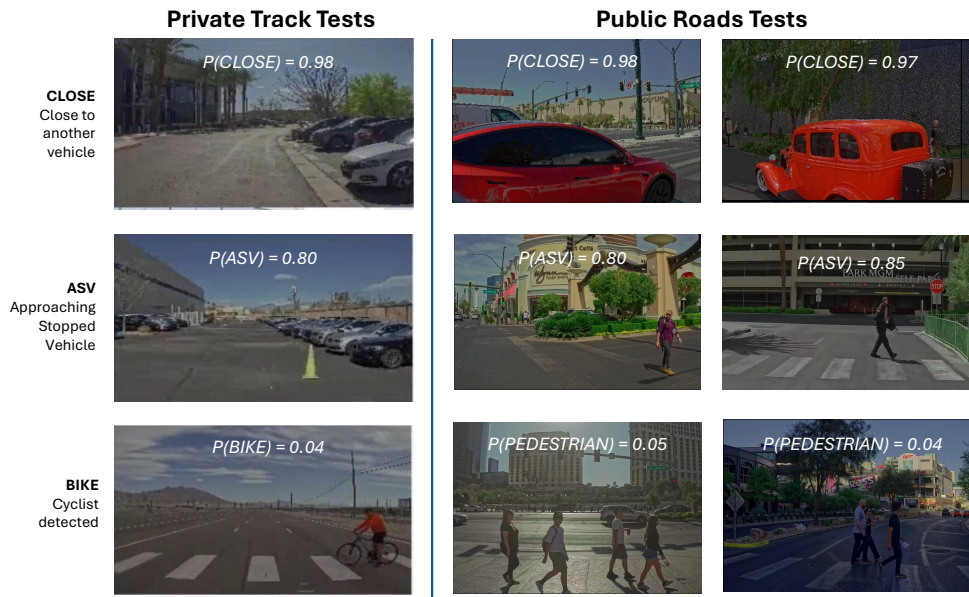


Fig. S10 Naturalistic scenario examples. The original surprising scenarios discovered on the private track and the analogous scenarios discovered on the public roads.

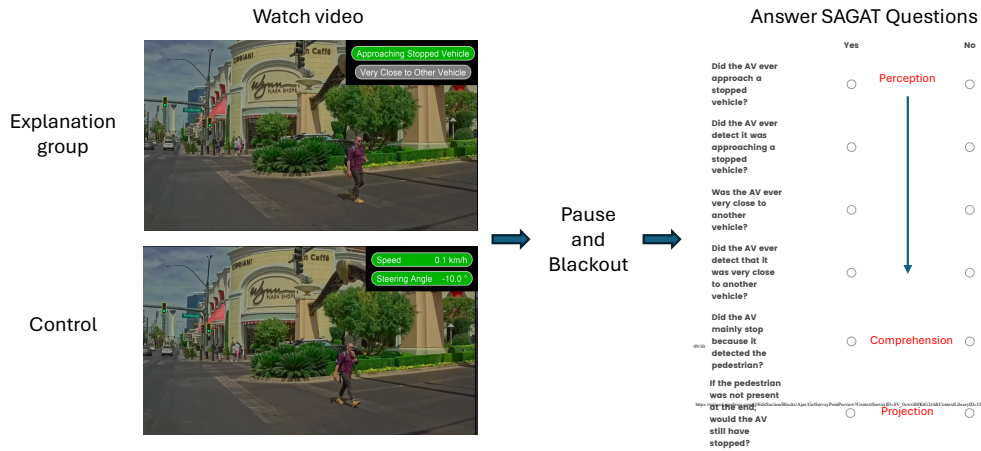


Fig. S11 SAGAT materials example. The two conditions (explanation vs. no explanation) were presented with the same video, followed by a “blackout”, and then 6 questions related to situational awareness.



Fig. S12 User materials example for the CLOSE concept, during a surprising and unsurprising event.



Fig. S13 User materials example for the ASV concept, during a surprising and unsurprising event.

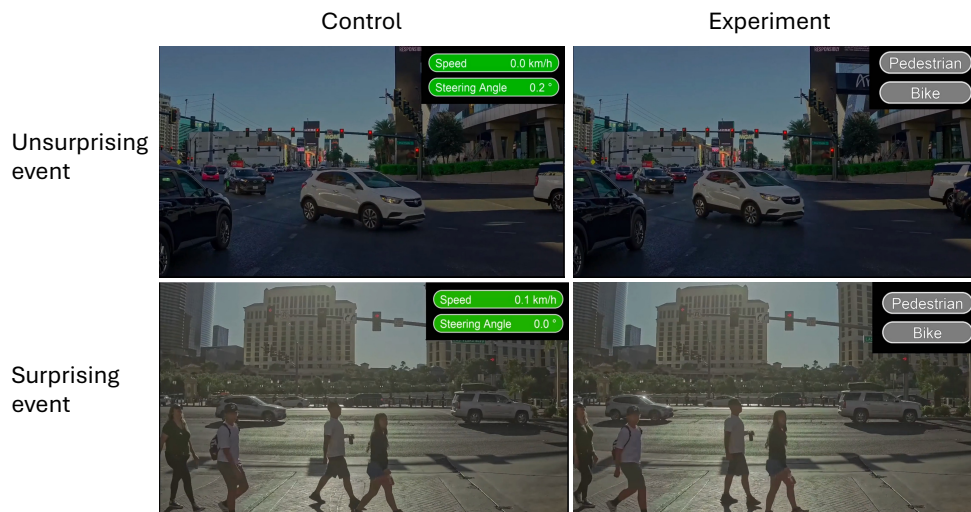


Fig. S14 User materials example for the PEDESTRIAN concept, during a surprising and unsurprising event.

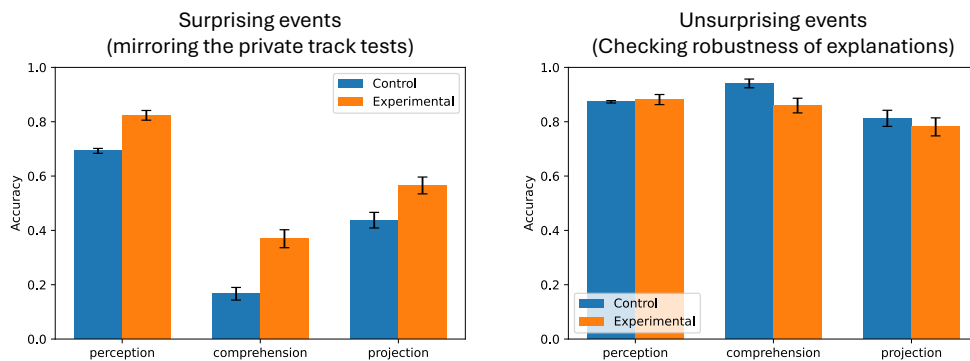


Fig. S15 Online SAGAT study results. Users in the experimental group reported significantly higher accuracy on perception, comprehension, and projection during surprising events. During unsurprising events, there were no significant differences. Although a negative trend was noted for comprehension in the experimental group, it did not reach significance after Bonferroni correction (see Table S7). Taken with the results of the mental model elicitation studies, which found counterfactual prediction accuracy correlated with mental model goodness, these SAGAT results strongly indicate the improvements in situational awareness were due to underlying improvements in user mental models of the AV.

FEATURE	Model 1	Model 2	Model 3
STOPPED	0.0862	0.0014	0.0324
SLOW	0.1575	0.0014	0.0324
FAST	0.1903	—	—
STOP SIGN	0.2368	—	—
TRAFFIC LIGHT	0.0938	—	—
INTERSECTION	0.0856	0.0247	0.0535
PEDESTRIAN	0.0998	—	—
FOLLOWING	0.1056	—	—
BIKE	0.1222	—	—
PUDO	0.2347	—	—
LEFT	—	0.0472	0.0332
RIGHT	—	0.0408	0.0410
STRAIGHT	—	0.0428	0.0592
ASV	—	0.0269	0.1050
CLOSE	—	0.0659	0.0702

Table S8 Negligible concept distribution shift: Wasserstein distances between the distribution of concept probabilities during the semi-naturalistic tests on the private track and the subsequent public-road test. Overall, the differences varied from mostly insignificant to low/medium in *STOP SIGN* and *PUDO*.